Journal of Sol-Gel Science and Technology 26, 605–608, 2003

Photoconductivity in Mesostructured Thin Films

G. VALVERDE, J. GARCÍA MACEDO*AND DANIEL CRUZ
Instituto de Fisica, UNAM, Apartado Postal 20-364, 01000 Mexico, D.F., Mexico
gamaj@fisica.unam.mx

J.I. ZINK AND R. HERNÁNDEZ
Department of Chemistry and Biochemistry, UCLA, Los Angeles, CA 90095
zink@chem.ucla.edu

Abstract. Mesostructured silica films are widely studied due to their different structures, properties and variety of possible applications. Sodium dodecyl sulfate (SDS)-templated sol-gel silica films possess highly ordered lamellar phase structure. It is expected that molecules and polymer chains line up with these layered structures when incorporated into the films. Mesostructured thin films were doped with Dispersed Red 1 (DR1) and carbazole (($(C_6H_4)_2NH$)). The films were poled by corona discharge at 120 C. Absorption spectra were recorded as function of the polarization time. Dependence of the absorption coefficient with polarization time was fitted with a Langevin-Debye equation. It shows a saturation level after 60 minutes of polarization. We compare the efficiency of mesostructured thin films with that of amorphous films. The photoconductivity technique was used to determine the charge transport mechanism of these films. From current density versus electrostatic applied field, the parameters for the photovoltaic effect and photoconductivity were determined. Results of the mesostructured thin films are also compared to those of $KNbO_3$ crystals.

Keywords: sol-gel, photoconductivity, mesostructure and thin films

Introduction

To synthesize these mesostructured silica thin films, four reagents are generally required: water, a surfactant, a silica source (such as TEOS), and a catalyst. Mesostructured silica films use surfactants to template or provide ordered structure to the amorphous silica matrix. The mesostructured thin films consist of two distinct regions: the 'framework' that is formed by the sol-gel metal oxide, and the 'organic' region that is formed by the template. When the template is an ionic surfactant (SDS), then an 'ionic' region will be formed at the interface between the organic and framework regions (Fig. 1). Molecules and polymer chains incorporated into the films can be expected to line up within the layer. This feature may allow electron transport from one end of the film to the other if the electron transferring species are densely aligned in the planes across the entire length of the film.

Dip coating in conjunction with surfactant-templating has been applied to the production of continuous, macroscopic films as thin as ~0.1 μm that contain long-range mesostructural order [1]. The potential applications for optical information processing and holographic image storage have been studied by photorefractive response on crystals [2] and amorphous materials [3]. In the past five years organic materials have emerged as an important new class of photorefractive media [4, 5]. The photorefractive effect can be evidenced from multifunctional materials that combine photosensitivity, photoconductivity, and electro-optic properties. The most commonly used charge transporting groups are carbazole units. We prepared sol-gel thin films by using the dip-coating technique with a

---

*To whom all correspondence should be addressed.

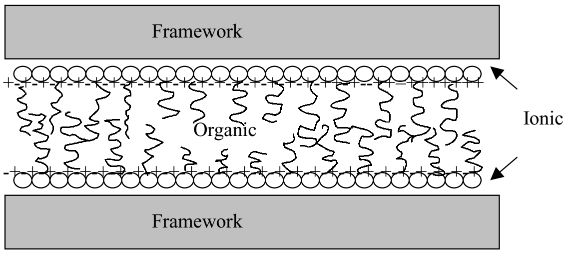

Figure 1. The spatial regions of a mesostructured film when the structure-directing agent is an ionic surfactant (SDS).

second-order chromophore (DR1) and a charge transporting molecule (carbazole).

Then, the dipole orientation of the nonlinear active chromophores was achieved by the single-point corona poling technique using a sharp metallic needle as electrode.

Photoconductivity studies on these films give information about the charge transport mechanism. It is important to determine the charge transport mechanism in order to improve the material properties for photorefractive applications. Improving the material properties can only be achieved by controlling the structure of these films.

Experimental

The sol was prepared by refluxing TEOS (Aldrich), ethanol, water and HCl (molar ratio: 0.14:0.52:0.13:3 × 10^{-3}) at 60°C for 90 min. This forms the stock solution [1, 6], designed to minimize the siloxane condensation rate. The hydrolysis was performed under acidic conditions with tetrahydrofuran (THF) as a common solvent. The molar concentration was defined as: DR1:SDS:SiK = [1:20:20]. Typically 0.1 ml of water, 0.4 ml of 0.07 N HCl, 15.7 ml of ethanol, 17 ml of THF, 0.046 g of DR1 and 0.5 g of carbazole were added to 3.3 ml of the stock solution. The sol was stirred for three days at room temperature.

The films were drawn with the equipment described previously that uses hydraulic motion to produce a steady and vibration-free withdrawal of the substrate from the sol [7]. The films were withdrawn at a speed of 5 cm/min.

The structure of the final films was characterized with X-ray diffraction (XRD) using Cu K_α radiation with $\lambda = 1.5418$ Å. The film was cut and polished to get a small sample, whose dimensions were 0.6 cm × 0.5 cm.

Optical absorption spectra were taken with a Perkin Elmer Lambda 900 Spectrophotometer. The sample was maintained in a 10^{-5} Torr vacuum cryostat at room temperature in order to avoid problems with humidity. Silver electrodes were painted on the sample prior to placing it in the cryostat. In order to measure photocurrents on the films they were illuminated with an Oriel 79309 10-mW He-Ne laser. Currents were measured with a 642 Keithley electrometer connected in series with the voltage power supply. The applied electrostatic field E was parallel to the thin film. Light intensity was measured at the sample position with a Spectra Physics 404 power meter [8]. DR1 molecules were oriented under Corona electric field poling at 120°C as function of time, and the field was taken away once the sample reached room temperature.

Results

Mesostructured silica films templated by SDS can be obtained by adding 0.86 gr of SDS to the TEOS sol. X-Ray diffraction (XRD) show peaks at $2\theta = 4.51°$ and 6.78°. They probably arise from packing of the hydrocarbon chains within the surfactant layers. The XRD patterns are most consistent with a lamellar-phase structure with alternating surfactant and silica layers [9]. The *d*-spacing was ~42 Å calculated from the position of the (001) peak for 2 wt% SDS films [1]. Mesostructured SDS sol-gel powders have also been reported to display lamellar structure with a *d*-spacing of 35 Å [10].

Absorption spectra evolution as a function of the poling time is illustrated in Fig. 2. A clear decrease is observed when the poling time increases. The absorption

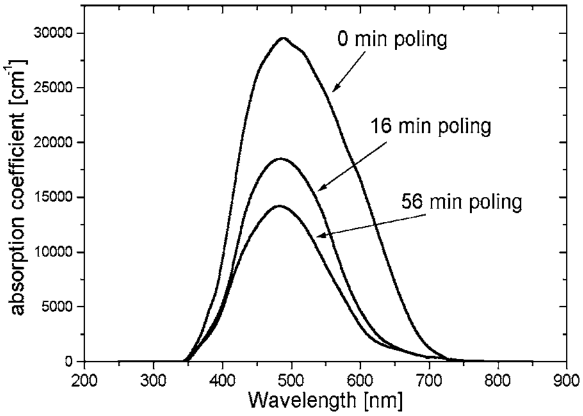

Figure 2. Absorption coefficient evolution with poling time.

coefficient compared with the initial one, changes continuously until saturation is reached after 60 minutes of poling.

Absorption diminished because the initial DR1 dipoles have a random orientation in the film plane. Due to the electric Corona Field, applied perpendicular to this plane, the molecules are orientated in the same direction. The electric field from the light reaching the sample during absorption measurements (that is contained in the film plane) sees less transversal dipoles as they become oriented, that is why the absorption diminishes when the poling time increases. With data from Fig. 2, the order parameter was calculated according to [11]:

$$\rho = 1 - \frac{A_\perp}{A_0}, \tag{1}$$

where $A_\perp$ (A_0) is normal absorption after (before) poling. Results are depicted in Fig. 3. This behavior is due to polarization saturation that follows the Langevin-Debye equation. Data satisfactorily fit this equation, as Fig. 3 shows (black line).

The molecular orientation is corroborated by the increment in the order parameter as a function of poling time, as it is shown in Fig. 3. The figure shows saturation after 2 hrs of poling with a 55% value, indicating there is an asymptotical polarization from the molecules. To date, this is the highest reported order value. Data from amorphous films made in France and studied at Mexico [12] are included in Fig. 3. As it is shown, the final order parameter is 57% higher in the mesostructured films, due to the lamellar structure.

Photoconductivity results are shown in Fig. 4. A straight line was easily fit to the data. This indicates an ohmic behavior. The slope from the illumination current curve is larger than the dark current curve at 16 minutes of polarization time. We also observed a change in the slope between the illuminated curve and the dark curve at zero minutes.

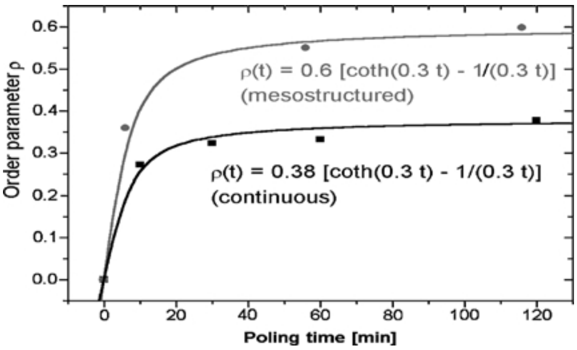

Figure 3. Order parameter evolution with poling time.

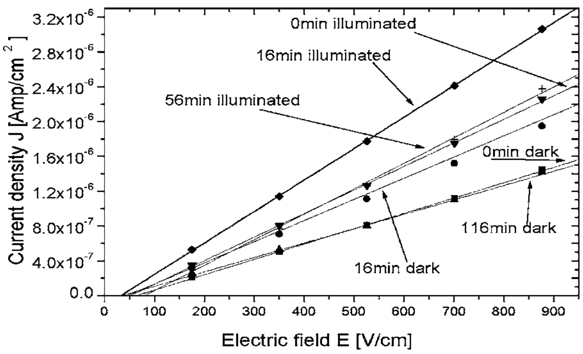

Figure 4. Dark and illuminated current curves for different poling times.

Charge transport in insulating materials is given by [8]:

$$j = e\phi l_0 \alpha I/h\nu + (en_0\mu + e\phi\mu\tau\alpha I/h\nu)E \tag{2}$$

The first term is the photovoltaic effect transport, the second one is the dark conductivity $\sigma = en_0\mu$, and the third one is the photoconductivity itself. In this equation, I is the light intensity with energy $h\nu$, ϕ is the quantum efficiency for exciting a free carrier, μ is the charge mobility, E is the applied electric field, α is the absorption coefficient, τ is the half life of the excited carriers, n_0 is the carrier density that produces dark conductivity and l_0 is the mean free path. With this equation, by measuring I, the dark conductivity and the conductivity under illumination, and fitting the data by least squares method, as it is shown in Fig. 3, the ϕl_0 and $\phi\mu\tau$ parameters are obtained. They are reported in Table 1. Their magnitudes are lower than those obtained in photorefractive crystals [8].

As it is shown in Fig. 4, conductivity increases with poling time until a maximum is reached, and then it decreases. This is better shown in Fig. 5, which illustrates the slope change from photoconductivity results. As it is observed, there is an optimal polarization time at approximately 35 minutes that produces the maximum conductivity response for both, dark conductivity and photoconductivity. We have observed the same result several times. Data are fitted by a gaussian equation (continuous lines). By considering the arguments from Takimoto et al. [13], working on films with oligo-p-phenylene sulfide, on which they observed that carriers were more easily transported perpendicular to the molecular chain axis than along that axis, we can

Table 1. Transport parameters.

	DR1 with carbazole		KNbO$_3$:Fe	
t (min)	ϕl_0 (cm × 10^{-11})	$\phi\mu\tau$ (cm^2/V × 10^{-11})	ϕl_0 (cm × 10^{-11})	$\phi\mu\tau$ (cm^2/V × 10^{-11})
0	6.63	0.23	850	23.38
6	8.29	0.15	–	–
16	3.87	0.46	–	–
56	20.97	0.22	–	–
116	19.54	0.16	–	–

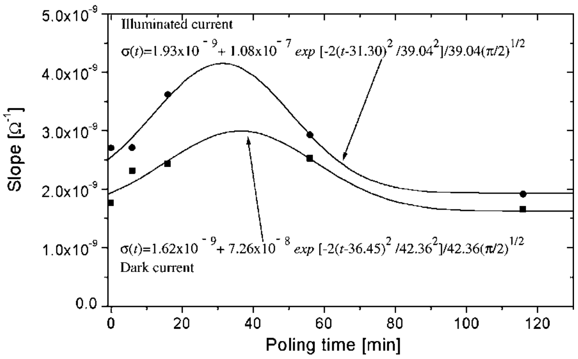

Figure 5. Slope of lines in Fig. 4, as a function of the poling time.

explain the photoconductivity increment with poling. According to these authors, when the molecules are oriented perpendicular to the film plane, the charge clouds from the π electrons in the molecules, are closer so they have a better chance to hop from one molecule to another, therefore increasing the photoconductivity. We should state that there is no clear explanation why there is an optimal poling time. More experiments are being conducted to clarify this point.

Conclusions

We produced mesostructured thin films doped with DR1 and SiK with highly ordered lamellar phase structure by dip-coating. These thin films exhibit photosensitivity under high electric field poling. The obtained values for photovoltaic and photoconductivity parameters are smaller then those from photorefractive crystals. Order parameter evolution with poling time follows a Langevin-Debye equation. The increment in conductivity with poling can be explained by the increase in π electron hopping when the molecules are oriented perpendicular to the plane of the film. The efficiency in our mesostructured thin films (55%) is 57% larger than those from amorphous films [12]. This is the highest reported value to date.

Akcnowledgments

This work has been supported by UCMEXUS, DGAPA UNAM IN103199 and CONACYT 34582-E.

References

1. M.H. Huang, B.S. Dunn, and J.I. Zink, Journal of the American Chemical Society **122**, 3739 (2000).
2. P. Gunter and J.P. Huignard, in *Topics in Applied Physics*, edited by P. Gunter and J.P. Huignard (Springer-Verlag, Berlin, 1989), p. 205.
3. F. Chaput, D. Riehl, J.P. Boilot, K. Cargnelli, M. Canva, Y. Levy, and A. Brun, Chemistry of Materials **8**, 312 (1996).
4. K. Sutter and P.J. Guenter, Journal of the Optical Society of America B **12**, 2274 (1990).
5. W.E. Moerner and S.M. Silence, Chemical Reviews **94**, 127 (1994).
6. C.J. Brinker et al., in *Access in Nanoporous Materials*, edited by T.J. Pinnavaia and M.F. Thorpe (Plenum, New York, 1995), p. 123.
7. F. Nishida, J.M. McKierman, B. Dunn, J.I. Zink, C.J. Brinker, and A.J. Hurd, Journal of American Ceramics Society **78**, 1640 (1995).
8. J. García M., M.A. Mondragon, J.M. Hernandez A., and J.L. Maldonado R., Optical Materials **3**, 61 (1994) .
9. Q. Huo, D.I. Margoleses, and G.D. Stucky, Chemical Materials **8**, 1147 (1996).
10. M. Yada, H. Kitamura, M. Machida, and T. Kijima, Langmuir **13**, 5252 (1997).
11. B.J. Tabor, E.P. Magre, and J. Boon, European Polymer Journal **7**, 1127 (1971).
12. J.A. Reyes-Esqueda, A. Franco, M. Bizarro, J. García M., M. Canva, B. Darracq, Y. Levy, K. Lahlil, F. Chaput, and J.P. Boilot, Journal of Sol-Gel Science and Technology **26**(1–3), 1011 (2003). XI Workshop Sol-Gel 2001.
13. A. Takimoto, H. Wakemoto, and H. Ogawa, Japanese Applied Physics **32**, 971 (1993).